

OPTIMAS: Optimizing Compound AI Systems with Globally Aligned Local Rewards

Shirley Wu^{*1}, Parth Sarthi^{*1}, Shiyu Zhao^{*1}, Aaron Lee¹, Adrian Mladenic Grobelnik³,
Herumb Shandilya¹, Nurendra Choudhary², Eddie Huang², Karthik Subbian²,
Linjun Zhang⁴, Diyi Yang¹, James Zou^{†1}, Jure Leskovec^{†1}

¹Stanford University ²Amazon ³Jožef Stefan Institute ⁴Rutgers University

*† Equal first / senior authors

<https://optimas.stanford.edu/>

Abstract

Compound AI systems integrating multiple components, such as Large Language Models, specialized tools, and traditional machine learning models, are increasingly deployed to solve complex real-world tasks. However, optimizing compound systems remains challenging due to their non-differentiable structures and diverse configuration types across components, including prompts, hyperparameters, and model parameters. To address this challenge, we propose OPTIMAS, a unified framework for effective optimization of compound systems. The core idea of OPTIMAS is to maintain one *Local Reward Function* (LRF) per component, each satisfying a *local-global alignment* property, *i.e.*, each component’s local reward correlates with the global system performance. In each iteration, OPTIMAS efficiently adapts the LRFs to maintain this property while simultaneously maximizing each component’s local reward. This approach enables independent updates of heterogeneous configurations using the designated optimization method, while ensuring that local improvements consistently lead to performance gains. We present extensive evaluations across five real-world compound systems to demonstrate that OPTIMAS outperforms strong baselines by an average improvement of 11.92%, offering a general and effective approach for improving compound systems.

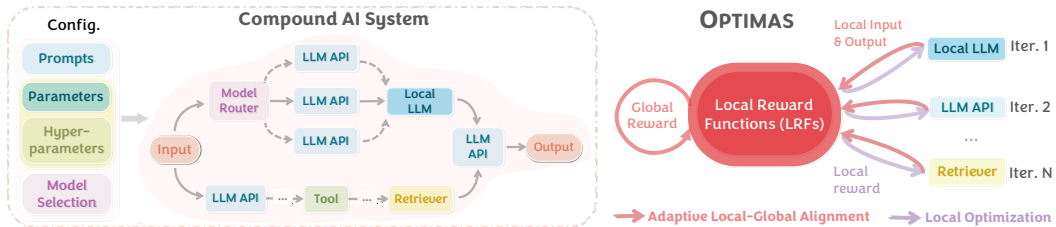


Figure 1: Overview. Given a compound AI system’s heterogeneous configurations (*e.g.*, prompts, parameters) across multiple components, OPTIMAS maintains globally aligned *Local Reward Functions* (LRFs) as the system evolves, where each supervises a component and assigns higher local rewards to outputs with higher system performance (*aka.* global rewards). It iteratively adapts LRFs and optimizes each component to maximize its local reward for effective system optimization.

1 Introduction

Modern AI systems increasingly employ compound systems that integrate multiple complex components, such as Large Language Models (LLMs), tool/function calls, and traditional machine learning models like retrievers [1–3]. These components collaborate to process heterogeneous data sources

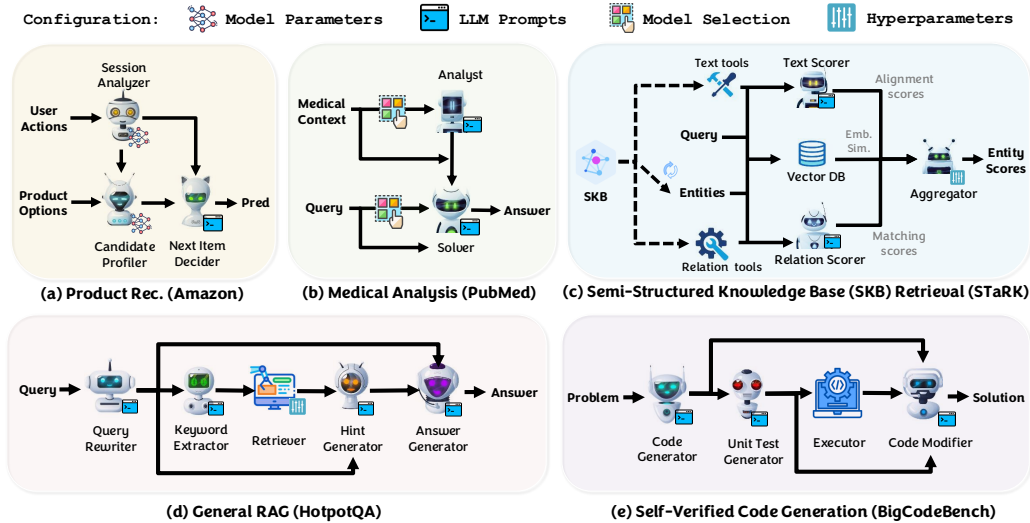


Figure 2: Five real-world and challenging compound AI systems. The goal is to automatically optimize the configuration across a heterogeneous set of components and parameters, *e.g.*, model parameters, prompts, model selection choice, and hyperparameters. See Appendix C for details.

and solve complex tasks through specialized subtask allocation [4–8]. While compound AI systems have yielded performance advantages over monolithic models [3, 9–12], they can be highly sensitive to the failure of individual components, which leads to cascading failures in the final results [13–16]. For example, if an LLM misinterprets an input query, it can retrieve irrelevant or misleading information. This leads to subsequent tool calls operating on incorrect inputs, producing unreliable outputs throughout the system. Therefore, optimizing these systems as a whole is crucial for maintaining reliability and system performance (*i.e.*, global rewards).

However, optimizing these compound AI systems end-to-end is fundamentally challenging due to their non-differentiable nature. Second, it is hard to jointly optimize heterogeneous configurations (textual *vs.* numerical, continuous *vs.* discrete) from individual components, including prompts, hyperparameters, model selections, and even model weights. Third, running the entire compound AI system during optimization to achieve global reward can be costly.

Previous works have largely focused on optimizing specific configurations in isolation, such as optimizing prompts through textual feedback [1, 2, 17–19] or model selection through iterative search [8, 20]. Yet these approaches can fail to capture critical bottlenecks—for example, a perfectly optimized prompt can struggle to compensate for a poorly chosen model. Furthermore, even individually well-optimized components may interact suboptimally, as outputs from one component optimized upstream might not have visibility into what a downstream component might need to improve the global reward. Moreover, such methods typically require costly system runs on many configurations, yielding low data efficiency.

Present work. Here we propose OPTIMAS (Figure 1), a unified framework for the effective and data-efficient optimization of compound AI systems. The core idea is to *learn a globally aligned Local Reward Function (LRF)* for each component, such that independently maximizing a component’s local reward still reliably improves the global rewards. We show that under mild conditions, our approach converges reliably, providing strong theoretical guarantees on optimization efficacy. Furthermore, since the learned LRFs can be used to optimized components locally, OPTIMAS has higher data efficiency by avoiding extensive runs of the entire compound AI system to achieve high global reward.

Specifically, each LRF estimates the contribution of its corresponding component’s output to the global reward. All LRFs are implemented using a shared LLM backbone, with separate projection heads for each component to produce component-specific rewards. We propose a **lightweight adaptation** mechanism using mini-batch preference data to ensure the LRFs remain aligned with the evolving system configuration (Figure 3). Leveraging its decentralized structure, OPTIMAS applies designated optimization method to each component based on its configuration type—for example, reinforcement learning for model parameters [21, 22] or metric-guided search for prompts and hyperparameters [17, 23, 24]. Overall, OPTIMAS iteratively updates heterogeneous configurations

Table 1: A comparison of OPTIMAS with selected methods. OPTIMAS optimizes compound systems with heterogeneous configurations and enables higher data efficiency with local optimization to reduce entire system runs. We prove OPTIMAS’s convergence under mild conditions.

	Supports compound system	Optimizes heterogeneous config.	Data efficiency	Convergence guarantee
OPRO [17]	✗	✗	✗	✗
DSPy [2]	✓	✗	✗	✗
TextGrad [1]	✓	✗	✗	✗
LLMSelector [8]	✓	✗	✗	✓
OPTIMAS	✓	✓	✓	✓

towards a higher global reward by using each adaptive LRF as an objective—optimizing a component to maximize its local reward, reducing the entire system runs to maintain higher data efficiency.

We conduct extensive experiments to evaluate OPTIMAS across five real-world compound systems (Figure 2), including challenging settings such as behavior-driven product recommendation and medical analysis. OPTIMAS consistently outperforms strong baselines, achieving an average relative improvement of 11.92% with higher data efficiency. While baseline methods occasionally improve performance—for example, DSPy improves the performance on the multi-hop QA system—they may degrade performance on other tasks, such as product recommendation. In contrast, OPTIMAS is the *only* method that improves performance across *all* five tasks, consistent with our theoretical guarantee (Section 4.4) that aligning local and global rewards enables effective optimization.

2 Related Work

Optimizing LLM single-step generation. Prior work extensively optimizes prompts for Large Language Models (LLMs) in single-step generation to improve performance [17, 18, 25–29], but these methods are limited in their ability to handle complex, multi-step tasks. For example, addressing complex queries often requires combining multiple components—such as LLMs, tools, and machine learning predictors—to obtain accurate predictions.

Optimizing multi-component/multi-step generation. Compound AI systems consisting of multiple components enable more complex planning and specialized processing at each task step [2, 30, 12, 3, 31]. Previous studies typically optimize different components separately, such as optimizing LLM prompts [2, 19, 1], fine-tuning model weights using supervised learning [32] or reinforcement learning [33, 34], developing model routing [8] and layer grouping[35] strategies, and selecting hyperparameters [36–39]. For example, LLMSelector [8] learns a lightweight policy to select the best LLM model for a given component at each step. However, optimizing only a *subset* of components might overlook critical bottlenecks to global reward. In contrast, OPTIMAS enables end-to-end optimization across *all* components.

Reward modeling for multi-step tasks. To provide more fine-grained supervision, recent works break down global rewards (*e.g.*, answer accuracy) into more targeted signals (*i.e.*, dense/process rewards). Representative approaches include leveraging or bootstrapping from human step-wise annotations [40–42]; hierarchical planning that assigns rewards to self-reflection and error correction steps [43]; using Monte Carlo Tree Search to assign credit to intermediate reasoning steps [44–48] or actions [49, 50]. The key insight of OPTIMAS is to maintain one globally aligned Local Reward Function (LRF) per component within an evolving compound system. Unlike prior work focused on differentiable single policy models, OPTIMAS adapts these LRFs to maintain local-global alignment in a non-differentiable, multi-component system, consistently improving the global reward. The local optimization also offers higher data efficiency compared to some existing approaches [1, 8, 32] that require extensive system runs. Moreover, we provide theoretical analysis to prove the convergence of our framework. In Table 1, we highlight our key contributions compared to closely related works.

3 Problem Formulation: Optimizing Compound AI Systems

Compound AI system. A compound AI system is represented as a directed acyclic graph $\mathcal{G} = (\mathcal{C}, \mathcal{E})$, where $\mathcal{C} = \{C_k\}_{k=1}^K$ is a set of K distinct components (task nodes) and \mathcal{E} is the set of all possible directed edges between components. A component of the compound system can be an LLM, a general

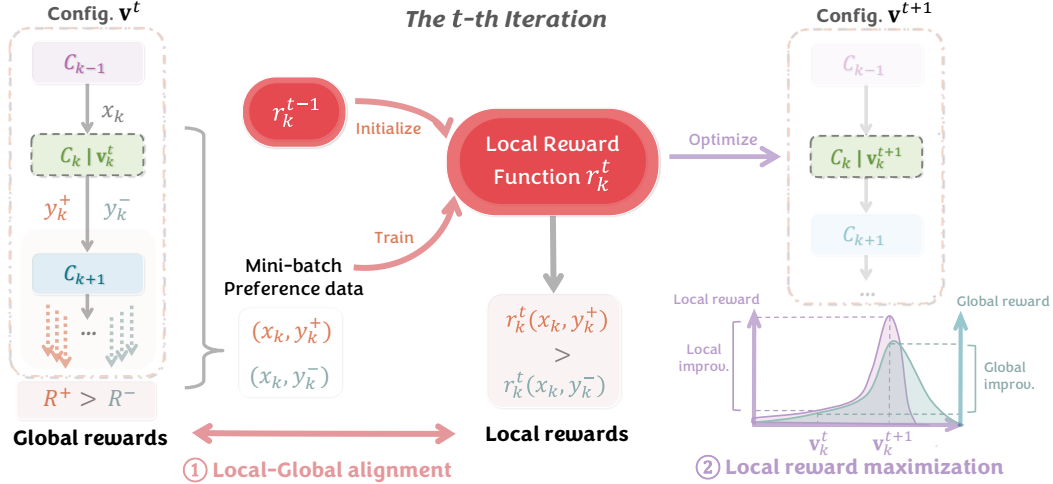


Figure 3: OPTIMAS optimization iteration. At each iteration, OPTIMAS updates a component C_k by first collecting a mini-batch of preference data and adapting its Local Reward Function r_k to remain aligned with the global task metric. This alignment helps ensure that optimizing the component to maximize its local reward also improves the global reward.

machine learning model, a model selector, *etc.* We denote the input and output to each component C_k as x_k and y_k , respectively. The system input is treated as a source node C_0 .

The system can operate with dynamic planning: for each input instance x , the connections $\mathcal{E}(x) \subseteq \mathcal{E}$ between the components can be adaptive. A directed edge $(C_i, C_j) \in \mathcal{E}(x)$ indicates that the output of component C_i is routed as input to component C_j when processing instance x . By default, we assume the component indices follow the topological order over \mathcal{E} , meaning that C_i is the upstream component of C_j if $i < j$.

Component configurations. A component $C_k : (x_k; \mathbf{v}_k) \mapsto y_k$ is controlled by a configuration policy \mathbf{v}_k . The configuration space \mathcal{V} can either be empty (indicating no optimizable configuration for the component), discrete (*e.g.*, textual prompts or model selections), or continuous (*e.g.*, model parameters or hyperparameters). We denote the joint configuration policy by $\mathbf{v} = (\mathbf{v}_1, \dots, \mathbf{v}_K)$.

Forward execution. For a given input x and configuration policy \mathbf{v} , the system executes components in topological order over the edge set $\mathcal{E}(x)$:

$$y_k = C_k(\{y_i \mid C_i \in pa(C_k)\}; \mathbf{v}_k), \quad (1)$$

where $pa(C_k)$ denotes all the parents of component C_k over $\mathcal{E}(x)$. For clarity, we define the overall system as $f(x; \mathbf{v}) := y$, where y is a collection of outputs from one or more components.

Optimization objective. Given a training dataset \mathcal{D} with system inputs and a user-defined global reward function $R : \mathcal{X} \times \mathcal{Y} \rightarrow \mathbb{R}$ that evaluates the final system output, the optimization goal is to find the configuration policy $\mathbf{v}^*(x)$ that maximizes the expected global reward:

$$\mathbf{v}^* = \arg \max_{\mathbf{v}} \mathbb{E}_{x \sim \mathcal{D}} [R(x, f(x; \mathbf{v}))]. \quad (2)$$

4 OPTIMAS: Globally Aligned Local Rewards for Optimization

Challenges. Directly optimizing the objective in Eq. (2) is difficult. As the configuration spaces are typically non-differentiable, gradient-based optimization cannot be used. Moreover, each policy \mathbf{v}_k may control a different configuration type, so the joint policy \mathbf{v} can span heterogeneous spaces. Therefore, previous efforts [1, 32, 8, 2] largely focus on optimizing the policy for single types of configurations, which simplifies the optimization problem; however, this also leads to suboptimal compound systems. Moreover, even with a single type of configurations, existing methods often require extensive runs on the system to search for better configurations, resulting in low data efficiency.

Key intuition. To address the above challenges, our approach (Figure 3) is to learn Local Reward Functions (LRFs) over individual components that align with the global reward, allowing independent optimization on heterogeneous components using different optimization approaches while improving the global reward. Since the optimization with LRFs is conducted locally, we reduce the number of entire system runs to achieve a high global reward.

Moreover, as the system configurations evolve over iterations, the LRFs should adapt to remain consistent with the updated configurations. Specifically, we introduce a *local-global alignment property* for learning LRFs (Section 4.1). To ensure alignment, OPTIMAS employs a *lightweight adaptation* mechanism that updates LRFs with minimal data sampled from the system, preserving consistency with the global reward (Section 4.2). These globally aligned LRFs enable each component to be effectively optimized through *local reward maximization* towards global reward gains (Section 4.3).

4.1 Learning Local Reward Functions

Definition (Local Reward Function (LRF)). An LRF on component C_k is defined as $r_k : (x_k, y_k) \rightarrow \mathbb{R}$, which evaluates the component’s output y_k given the provided context, such as the input x_k and an optional component task description.

Practical implementation. In practice, we implement all LRFs with a single LLM backbone ϕ and separate linear heads h_k , one head per component C_k for components with non-empty configurations. The backbone encodes the concatenated text inputs $[x_k, y_k]$ into an embedding, and the corresponding head projects this embedding to a scalar reward value. Therefore, each LRF is modeled by

$$r_k(x_k, y_k) = h_k \circ \phi([x_k, y_k]), \quad \text{for all } k \text{ if } \mathbf{v}_k \text{ is non-empty.} \quad (3)$$

We represent the LRFs as one multitask network to reduce computation and memory costs while maintaining the capacity to produce component-specific rewards.

Property (Local–global alignment). An LRF r_k is said to be *aligned* with the global reward R if, for every input x and for any two candidate outputs y_k^+, y_k^- of C_k ,

$$\begin{aligned} r_k(x_k, y_k^+) &\geq r_k(x_k, y_k^-) \\ \implies \mathbb{E}_{\text{downstream}} \left[R(x, f(x; \mathbf{v}_{-k}) \mid y_k^+) \right] &\geq \mathbb{E}_{\text{downstream}} \left[R(x, f(x; \mathbf{v}_{-k}) \mid y_k^-) \right], \end{aligned} \quad (4)$$

where \mathbf{v}_{-k} denotes the configurations of all *downstream* components—those that receive, directly or indirectly, information originating from C_k . The expectation term, which denotes the expected global reward for each candidate output, is estimated via Monte Carlo sampling. This involves executing the downstream components with the candidate output fixed, capturing their stochasticity, and averaging the resulting global rewards from the final system outputs.

Objective of reward functions. To obtain LRFs that conform to the local-global alignment property, we train each r_k using a pairwise log-sigmoid ranking loss:

$$\mathcal{L}_k(\mathcal{D}_k(\mathbf{v})) = -\mathbb{E}_{(x_k, y_k^+, y_k^-) \sim \mathcal{D}_k(\mathbf{v})} \left[\log \sigma(r_k(x_k, y_k^+) - r_k(x_k, y_k^-)) \right], \quad (5)$$

where $\mathcal{D}_k(\mathbf{v})$ is a preference dataset collected under the current system configuration \mathbf{v} .

To generate the preference dataset for each component C_k , we 1) execute the compound system up to C_k and record the partial trajectory $\langle x, (x_1, y_1), \dots, (x_{k-1}, y_{k-1}) \rangle$; 2) sample two candidate outputs for C_k (e.g., via higher-temperature decoding or alternate hyperparameters); and 3) estimate their expected task metrics according to the expectation terms on the right-hand side of Eq. (4). The output with the higher expected value is labeled as y_k^+ , and the other as y_k^- in $\mathcal{D}_k(\mathbf{v})$.

4.2 Adaptive Local Reward Functions via Offline-Online Training

Problem: Misaligned LRFs in the evolving system. As the system configuration evolves during optimization, LRFs trained under a previous configuration \mathbf{v}^t may become inaccurate under the updated configuration \mathbf{v}^{t+1} . For example, after updating a component C_k , the same upstream outputs may lead to different final outcomes, making earlier reward estimates inaccurate. Meanwhile, downstream components now receive inputs generated by the updated C_k , which may fall outside the distribution seen by their LRFs. These shifts accumulate over time, degrading the local–global alignment property (Eq. 4) that LRFs are designed to satisfy.

However, retraining all LRFs from scratch after every configuration update lowers the data efficiency due to the system runs involved to minimize Eq.4. To address this, we develop a lightweight adaptation strategy that incrementally refines the LRFs as the system evolves, maintaining alignment without full retraining.

Offline reward modeling. Given the initial system configuration \mathbf{v}^0 and input dataset \mathcal{D} , we first construct an offline preference dataset for each component and train its corresponding LRF to convergence. This offline phase establishes well-aligned LRFs that accurately reflect each component’s contribution to the global task metric, based on the input and output distribution of the components, providing a reliable foundation for subsequent optimization.

Online reward function adaptation. We sample a small input batch from \mathcal{D} and construct a mini-batch of preference data \mathcal{B}_k for C_k using the procedure described in Section 4.1. Therefore, we optimize the LRF on C_k on the objective:

$$\mathcal{L}_k^{\text{adapt}}(\mathcal{B}_k) = \mathcal{L}_k(\mathcal{B}_k) \quad (6)$$

This adaptation helps maintain the local–global alignment property (Eq. 4). Optionally, we can maintain a buffer of previous generated preference data for C_k into \mathcal{B}_k to enable stable optimization.

4.3 Optimization with Globally aligned Local Reward Functions

Given a globally aligned LRF r_k , we perform local optimization on each component C_k to improve its configuration \mathbf{v}_k . Specifically, we solve:

$$\mathbf{v}_k^{t+1} = \arg \max_{\mathbf{v}_k \in \mathcal{V}_k} \mathbb{E}_{x_k} [r_k(x_k, C_k(x_k; \mathbf{v}_k))] \quad \text{subject to} \quad d(\mathbf{v}_k, \mathbf{v}_k^t) \leq \delta, \quad (7)$$

where \mathbf{v}_k^t is the configuration before the t -th iteration, $d(\cdot, \cdot)$ is a distance function over configurations, and δ defines a trust region that bounds allowable updates. This constraint ensures that r_k is used within a region where it is expected to produce reliable evaluations.

In practice, explicitly setting the trust region threshold δ can be difficult due to heterogeneous configuration types (*e.g.*, continuous weights *vs.* discrete tokens). Instead, we adopt a conservative number of update steps to restrict the magnitude of change during each iteration.

Local Optimization. Since each LRF is associated with a specific component, OPTIMAS can flexibly apply a specialized optimization method for each component. Further implementation details are provided in Appendix E. Concisely,

- For textual prompts, we use prompt optimization algorithms such as OPRO [17] that ranks candidate prompts by their average local reward and select the best-performing one.
- For components that are trainable models (*e.g.*, an LLM), we apply reinforcement learning—such as Proximal Policy Optimization (PPO) [22]—using the LRF as the critic.
- For discrete or low-dimensional continuous configurations, such as model selection or hyperparameter tuning, we construct a probability distribution over candidate values based on their local rewards and sample from it to update the configuration.

Summary (Figure 3). OPTIMAS leverages offline training to learn a set of LRFs that are well-aligned with the global reward under the initial system configuration. During optimization, OPTIMAS iteratively conducts local optimization to update individual component configurations with high data efficiency, and adapts the corresponding LRFs to align with the evolving system using minimal data.

4.4 Theoretical Insights

We prove that the local–global alignment property (4) holds for the LRFs constructed in Section 4.1.

Theorem 4.1 (Informal). *Under regularity conditions, the maximizer of (5) satisfies the local-global alignment property (4). In addition, maximizing $r_k(x_k, C_k(x_k; \mathbf{v}_k))$ over \mathbf{v}_k and maximizing $R(x, f(x; \mathbf{v}_{-k}) \mid C_k(x_k; \mathbf{v}_k))$ over \mathbf{v}_k will yield the same solution.*

We defer the formal statement for this theorem to appendix A. Since solving (2) is generally challenging, below we introduce some regularity conditions to make the convergence analysis tractable.

Table 2: Performances of each method on the compound systems. The best and second-best results in each column are highlighted. Relative improvement is computed with respect to the best baseline.

	AMAZON Product Rec. (Acc.)	PUBMEDQA Medical Analysis (Acc.)	STARK-PRIME Complex Retrieval (MRR)	HOTPOTQA RAG (F1)	BIGCODEBENCH Verified Code Gen. (Pass Rate)
Unoptimized	21.21±3.78	57.46±0.75	40.73±0.64	33.80±1.51	36.67±1.35
LLMSelector	-	67.93±0.09	-	-	-
HBC	21.55±2.07	58.80±0.58	36.95±0.59	21.16±0.97	27.78±2.08
TextGrad	20.88±3.53	56.96±2.24	41.31±1.67	24.86±1.19	35.71±0.10
DSPy	18.18±0.82	60.26±0.40	41.40±0.04	44.90±0.32	33.81±2.75
OPTIMAS	24.24±0.82	69.13±0.33	50.54±0.70	50.48±1.48	38.92±0.36
Rel. Improv.	14.3%	1.8%	22.1%	12.4%	9.0%

Table 3: Number of equivalent runs on the entire systems (in thousands) by TextGrad, DSPy, and OPTIMAS in Table 2. We control the optimization process of each to use comparable system runs.

	AMAZON	PUBMEDQA	STARK-PRIME	HOTPOTQA	BIGCODEBENCH	Average
TextGrad	0.32	0.70	0.70	2.12	0.18	0.80
DSPy	0.24	0.66	0.66	2.09	0.28	0.79
OPTIMAS	0.31	0.52	0.51	2.02	0.21	0.71

As the configurations \mathbf{v} are heterogeneous, where some of the coordinates are discrete, and some are continuous, without loss of generality, we assume the first M configurations $\mathbf{v}^{(1)} = \{\mathbf{v}_1, \dots, \mathbf{v}_M\}$ are continuous, and the last $(K - M)$ configurations $\mathbf{v}^{(2)} = \{\mathbf{v}_{M+1}, \dots, \mathbf{v}_K\}$ are discrete. We write the objective function $\mathbb{E}_{x \sim \mathcal{D}} [R(x, f(x; \mathbf{v}))]$ as $l(\mathbf{v}) = l(\mathbf{v}_1, \mathbf{v}_2, \dots, \mathbf{v}_K) := l(\mathbf{v}^{(1)}, \mathbf{v}^{(2)})$.

Assumption 4.1. *Suppose for any given configuration $\mathbf{v}^{(2)}$, the initial level set $\{\mathbf{v}^{(2)} : l(\mathbf{v}^{(1)}, \mathbf{v}^{(2)}) \leq l(\mathbf{v}^{0,(1)}, \mathbf{v}^{(2)})\}$ is a compact set, where $\mathbf{v}^{0,(1)}$ is the initialization used in the algorithm for $\mathbf{v}^{(1)}$. In addition, for every component k and every fixed \mathbf{v}_{-k} , $l(\cdot, \mathbf{v}_{-k})$ has a unique maximizer.*

Theorem 4.2. *Under Assumption 4.1, the algorithm will converge to the component-wise maximum, that is, the limit point \mathbf{v}^* satisfies*

$$l(\mathbf{v}^*) \geq l(\mathbf{v}_k, \mathbf{v}_{-k}^*),$$

for any $k \in [K]$ and any \mathbf{v}_k .

In fact, our theoretical analysis shows that by conducting local optimization, OPTIMAS is essentially performing coordinate maximization. Therefore, existing convergence results for coordinate maximization directly apply. For instance, if the objective function additionally satisfies the Polyak–Łojasiewicz (PL) condition, the algorithm is guaranteed to converge to the global maximum.

5 Experiments

We evaluate OPTIMAS against five baselines on five real-world compound AI systems across diverse domains, aiming to validate its ability to improve system performance. Below, we summarize the dataset settings, baselines, and evaluation metrics, with further details provided in the appendix.

Benchmarks & Evaluation (Appendix B). We briefly introduce the benchmarks and task metrics.

- **AMAZON** [51]: A behavior-driven recommendation task based on Amazon product interactions, evaluated using accuracy to measure if the predicted next item matches the ground-truth item.
- **PUBMEDQA** [52]: A clinical classification dataset derived from PubMed abstracts [53], evaluated by accuracy, defined as the proportion of predictions that exactly match the ground-truth labels.
- **STARK-PRIME** [54]: A retrieval benchmark over semi-structured biomedical corpora, evaluated using Mean Reciprocal Rank (MRR), which averages the inverse rank of the first correct answer.
- **HOTPOTQA** [55]: A multi-hop question answering dataset, evaluated using the F1 score between predicted and ground-truth answers.
- **BIGCODEBENCH** [56]: The instruction split of BigCodeBench for self-verifying code generation, evaluated using pass rate: the percentage of final generated programs that pass the unit tests.

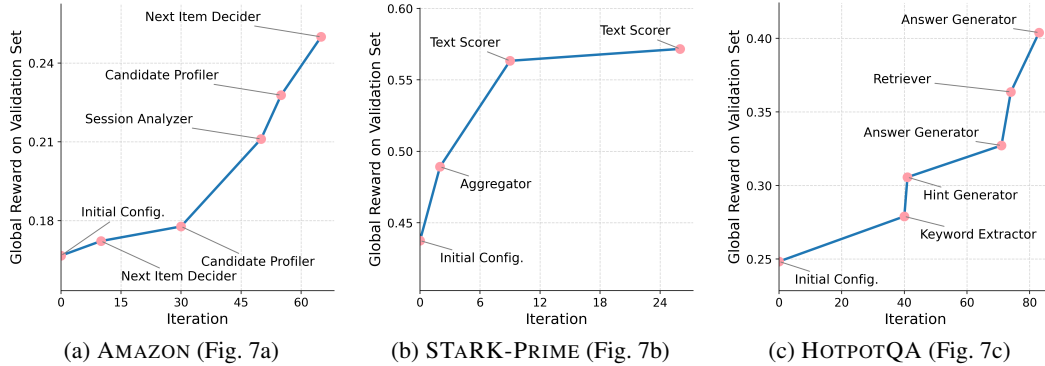


Figure 4: Global reward of the three compound AI systems over local optimization iterations. For conciseness, we show only the steps of local optimization that lead to an increase in global reward on the validation sets. The annotations indicate the components optimized at each step.

Table 4: Average pairwise ranking accuracy on validation sets, measuring how often the method assigns a higher score to the output with higher expected global reward.

	AMAZON	PUBMEDQA	STARK-PRIME	HOTPOTQA	BIGCODEBENCH	Avg.
LLM Judge (20-shot)	51.25%	49.54%	54.37%	50.00%	42.45%	49.52%
OPTIMAS	84.93%	65.28%	76.64%	72.40%	90.57%	77.96%

Compound Systems (Figure 2, *cf.* Appendix C). We design a compound system per benchmark with diverse and common patterns for agentic systems¹. All systems are accessible in our code repository.

Baselines (Appendix D). We compare OPTIMAS against five comprehensive baselines:

- **Unoptimized**: This system uses default settings for all components without any optimization.
- **LLMSelector** [8]: A lightweight policy selects the best LLM per component via model routing, without updating prompts or other variables. This method is only applicable on PUBMEDQA.
- **Hierarchical Behavior Cloning (HBC)** [57]: A hierarchical imitation learning approach that optimizes each component to produce outputs similar to those that lead to high global rewards.
- **TextGrad** [1]: A gradient-based prompt tuning method using estimated gradients from black-box LLMs to improve prompt efficacy.
- **DSPy** [2, 23]: A prompt optimization framework using the MIPRO algorithm that jointly refines module-level instructions and few-shot demonstrations.

5.1 Final Global Reward and Optimization Dynamics

Consistent Gains vs. Strong Baselines (Table 2). We compare OPTIMAS with the baselines under similar numbers of system runs. Under this controlled data cost (Table 3), OPTIMAS consistently improves global rewards across all five compound systems, achieving an average relative improvement of 11.92% compared to the best baseline.

While the strong baseline DSPy shows notable improvements on some datasets—for instance, a 21.6% gain on HOTPOTQA—their performance may be inconsistent and can even degrade the system—a 14.3% drop on the AMAZON dataset. For LLMSelector, the total system runs cost is 2.8k which is 3x more expensive than OPTIMAS. The comparison highlights the advantage of using globally aligned reward functions to guide local optimization.

Progressive gains during OPTIMAS optimization (Figure 4). Further, we visualize the changes in global reward across optimization iterations. Within a small number of iterations, OPTIMAS achieves a substantial average improvement of 41.7% over the initial global reward on the validation sets, using lightweight and data-efficient updates. Specifically, by updating each component during local optimization, OPTIMAS approximates the optimal system configuration. Full configuration traces are provided in Appendix E.

¹<https://www.anthropic.com/engineering/building-effective-agents>

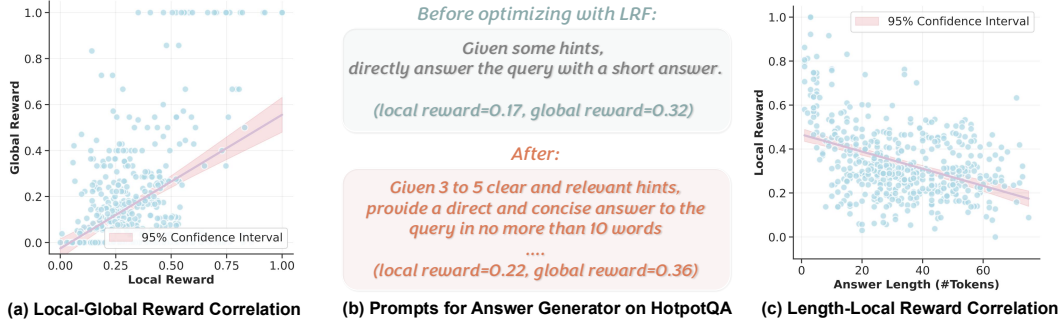


Figure 5: Case Study on HOTPOTQA: (a) Before local optimization, we collect outputs from Answer Generator, where we compute each output’s local reward from LRF and global reward, demonstrating that the local reward highly correlates with the global reward. (b) OPTIMAS optimizes prompts on Answer Generator to maximize local rewards, achieving higher global reward. (c) Interpretation: LRF learns to prefer concise answers from the local-global alignment.

5.2 In-depth Study of OPTIMAS

We analyze OPTIMAS to provide insights and understand how its core mechanism—local-global alignment—contributes to improvements in overall system global reward.

(1) The quality of local-global alignment (Table 4). To assess alignment quality, we compute pairwise ranking accuracy: the probability that an output with higher global reward receives a higher local reward than an output with lower global reward. This metric reflects how well the learned LRFs aligns with global rewards. We compare against a baseline, LLM Judge, which prompts a gpt-4o model to rank outputs based on 20 in-context input-output examples—10 associated with high global rewards and 10 with low global rewards. This approach resembles prior methods such as TextGrad, which rely on few-shot reasoning over textual patterns.

In Table 4, LLM Judge performs closer to random guessing, likely due to the diversity and stochasticity of intermediate outputs in compound systems. These factors make it difficult to infer output quality based solely on static textual patterns. In contrast, the learned LRFs achieve a substantially higher average pairwise accuracy of 77.96%, indicates the quality of the local reward produced by our LRFs compared to textual reasoning. Moreover, LRFs are trained to internalize the local-global alignment within their weights, eliminating the reliance on limited in-context examples or textual patterns, and enabling more precise alignment with global reward.

(3) Insights learned by LRFs during local-global alignment (Figure 5). We examine the LRF learned for the Answer Generator in the HOTPOTQA system. Figure 5(a) shows a positive correlation between the local reward and global reward of each predicted answer, indicating that our LRF captures how each local output contributes to the global reward.

Figure 5(b) illustrates how local optimization with LRF refines the prompt. Initially, the prompt instructs the generator to “*directly answer the query with a short answer,*” yielding a local reward of 0.17 and a global reward of 0.32. After optimization with LRF, the instruction becomes more specific: “*concise answer to the query in no more than 10 words ...*,” increasing the local reward to 0.22 and the global reward to 0.36. This improvement can be attributed to the clear negative correlation between answer length and local reward, as shown in Figure 5(c), where shorter responses tend to be rewarded more. Since correct answers in HotpotQA are often concise, this correlation naturally guides the system to enforce brevity through prompt optimization.

(3) Correlation between alignment quality and global reward (Figure 6 (a) and (b)). To better understand how alignment quality affects global reward, we conduct controlled experiments on the AMAZON and HOTPOTQA systems. For each system, we select a key component (Candidate Profiler for AMAZON and Answer Generator for HOTPOTQA) and train local reward models with varying alignment quality, measured by pairwise ranking accuracy. Pairwise ranking accuracy quantifies how often an output with higher global reward is assigned a higher local reward compared to an output with lower global reward.

We then perform single-step local optimization using each trained model and measure the average global reward achieved after updating only that component. Figure 6 shows a strong positive correla-

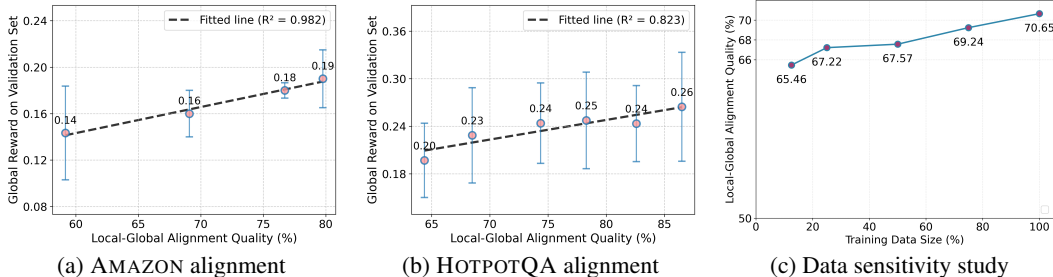


Figure 6: **Part 1:** Correlation between alignment quality and global reward on (a) AMAZON and (b) HOTPOTQA. Local reward models with varying alignment quality—measured by pairwise ranking accuracy—are used to optimize selected components; a strong positive correlation is observed, with higher alignment consistently yielding larger global reward gains. **Part 2:** Impact of training-data size on evaluation accuracy for HOTPOTQA (c). OPTIMAS remains robust even with limited data, showing only a 5.19% absolute drop when trained on just 12.5% of the data compared with the full dataset, demonstrating efficient data usage.

tion between the alignment quality of the local reward model and the corresponding improvement in global reward. Specifically, local reward models with higher alignment quality consistently produce larger global reward gains, underscoring that accurate local-to-global alignment is critical for effective and reliable local optimization. Conversely, lower-aligned local rewards may misguide optimization and lead to negligible or even negative improvements in global reward.

(4) Ablation on Data Size (Figure 6 (c)). To evaluate the data efficiency of OPTIMAS, we examine how the amount of training data (system runs) affects the performance of learned LRFs. We train local reward models on the HOTPOTQA system using varying percentages of available training data: 12.5%, 25%, 50%, 75%, and 100%. Each model is trained for 3 epochs, and performance is measured by pairwise ranking accuracy—how often an output with higher global reward is assigned a higher local reward compared to an output with lower global reward.

OPTIMAS maintains reasonable performance across different data sizes. Even with only 12.5% of the data, the system achieves 65.46% accuracy (92.7% of full-data performance), while 25% of the data yields 67.22% accuracy (95.1% of full-data performance). The diminishing returns beyond 25% data suggest that the core patterns for local-global alignment can be captured efficiently from limited preference data. This data efficiency is particularly valuable in practice, where collecting extensive preference data through system runs can be computationally expensive. Combined with the reduced computational cost of local optimization, these results demonstrate that OPTIMAS provides a practical solution for optimizing complex compound AI systems even in resource-constrained environments.

6 Conclusion

We presented OPTIMAS, a unified framework to optimize compound AI systems end-to-end. Its key insight is to maintain one *Local Reward Function* per component, aligned with the system’s global performance. This design allows every component, whether a fine-tunable LLM, API-based LLM, tool hyperparameters, or model selection, to be optimized locally while still improving the overall system. Through extensive experiments on five real-world tasks, we demonstrated that *globally aligned local optimization* outperforms strong baselines, including specialized prompt-tuning, hierarchical behavior cloning, and model selection approaches. While our approach effectively reduces system-wide runs, a current limitation is that we choose which component to optimize using a simple gap-based heuristic; developing a more principled or learned scheduler for selecting both the component is an important direction for future work. We believe OPTIMAS will serve as a general, data-efficient approach for continually refining multi-component AI systems in diverse application domains.

References

- [1] Mert Yuksekgonul, Federico Bianchi, Joseph Boen, Sheng Liu, Pan Lu, Zhi Huang, Carlos Guestrin, and James Zou. Optimizing generative ai by backpropagating language model feedback. *Nature*, 639:609–616, 2025.
- [2] Omar Khattab, Keshav Santhanam, Xiang Lisa Li, David Hall, Percy Liang, Christopher Potts, and Matei Zaharia. Demonstrate-search-predict: Composing retrieval and language models for knowledge-intensive nlp, 2023.
- [3] Yilun Du, Shuang Li, Antonio Torralba, Joshua B. Tenenbaum, and Igor Mordatch. Improving factuality and reasoning in language models through multiagent debate. *arXiv*, 2023.
- [4] Matei Zaharia, Omar Khattab, Lingjiao Chen, Jared Quincy Davis, Heather Miller, Chris Potts, James Zou, Michael Carbin, Jonathan Frankle, Naveen Rao, and Ali Ghodsi. The shift from models to compound ai systems. <https://bair.berkeley.edu/blog/2024/02/18/compound-ai-systems/>, 2024.
- [5] Han Zhou, Xingchen Wan, Ruoxi Sun, Hamid Palangi, Shariq Iqbal, Ivan Vulic, Anna Korhonen, and Sercan Ö. Arik. Multi-agent design: Optimizing agents with better prompts and topologies. *CoRR*, abs/2502.02533, 2025.
- [6] Jan Leike, David Krueger, Tom Everitt, Miljan Martic, Vishal Maini, and Shane Legg. Scalable agent alignment via reward modeling: a research direction. *CoRR*, abs/1811.07871, 2018. URL <http://arxiv.org/abs/1811.07871>.
- [7] Eser Kandogan, Nikita Bhutani, Dan Zhang, Rafael Li Chen, Sairam Gurajada, and Estevam Hruschka. Orchestrating agents and data for enterprise: A blueprint architecture for compound ai, 2025. URL <https://arxiv.org/abs/2504.08148>.
- [8] Lingjiao Chen, Jared Quincy Davis, Boris Hanin, Peter Bailis, Matei Zaharia, James Zou, and Ion Stoica. Optimizing model selection for compound ai systems, 2025.
- [9] Dong Huang, Qingwen Bu, Jie M. Zhang, Michael Luck, and Heming Cui. Agentcoder: Multi-agent-based code generation with iterative testing and optimisation. *CoRR*, abs/2312.13010, 2023.
- [10] Rémi Leblond and et al. Alphacode 2 technical report. Technical report, DeepMind, 2023.
- [11] Patrick Lewis, Ethan Perez, Aleksandra Piktus, Fabio Petroni, Vladimir Karpukhin, Naman Goyal, Heinrich Küttler, Mike Lewis, Wen-tau Yih, Tim Rocktäschel, Sebastian Riedel, and Douwe Kiela. Retrieval-augmented generation for knowledge-intensive NLP tasks. In *NeurIPS*, 2020.
- [12] Zijun Liu, Yanzhe Zhang, Peng Li, Yang Liu, and Diyi Yang. Dynamic llm-agent network: An llm-agent collaboration framework with agent team optimization. *arXiv*, 2023.
- [13] Mert Cemri, Melissa Z. Pan, Shuyi Yang, Lakshya A. Agrawal, Bhavya Chopra, Rishabh Tiwari, Kurt Keutzer, Aditya Parameswaran, Dan Klein, Kannan Ramchandran, Matei Zaharia, Joseph E. Gonzalez, and Ion Stoica. Why do multi-agent llm systems fail?, 2025. URL <https://arxiv.org/abs/2503.13657>.
- [14] Jen tse Huang, Jiaxu Zhou, Tailin Jin, Xuhui Zhou, Zixi Chen, Wenxuan Wang, Youliang Yuan, Michael R. Lyu, and Maarten Sap. On the resilience of llm-based multi-agent collaboration with faulty agents, 2025. URL <https://arxiv.org/abs/2408.00989>.
- [15] Jingyu Peng, Maolin Wang, Xiangyu Zhao, Kai Zhang, Wanyu Wang, Pengyue Jia, Qidong Liu, Ruocheng Guo, and Qi Liu. Stepwise reasoning error disruption attack of llms, 2025. URL <https://arxiv.org/abs/2412.11934>.
- [16] Angelica Chen, Jason Phang, Alicia Parrish, Vishakh Padmakumar, Chen Zhao, Samuel R. Bowman, and Kyunghyun Cho. Two failures of self-consistency in the multi-step reasoning of llms, 2024. URL <https://arxiv.org/abs/2305.14279>.

- [17] Chengrun Yang, Xuezhi Wang, Yifeng Lu, Hanxiao Liu, Quoc V. Le, Denny Zhou, and Xinyun Chen. Large language models as optimizers. In *ICLR*, 2024.
- [18] Aman Madaan, Niket Tandon, Prakhar Gupta, Skyler Hallinan, Luyu Gao, Sarah Wiegrefe, Uri Alon, Nouha Dziri, Shrimai Prabhunoye, Yiming Yang, Shashank Gupta, Bodhisattwa Prasad Majumder, Katherine Hermann, Sean Welleck, Amir Yazdanbakhsh, and Peter Clark. Self-refine: Iterative refinement with self-feedback. In *NeurIPS*, 2023.
- [19] Shirley Wu, Shiyu Zhao, Qian Huang, Kexin Huang, Michihiro Yasunaga, Kaidi Cao, Vassilis N. Ioannidis, Karthik Subbian, Jure Leskovec, and James Zou. Avatar: Optimizing llm agents for tool usage via contrastive reasoning. *NeurIPS*, 2024.
- [20] Lingjiao Chen, Matei Zaharia, and James Zou. Frugalgpt: How to use large language models while reducing cost and improving performance. *Transactions on Machine Learning Research*, 2024.
- [21] Rafael Rafailov, Archit Sharma, Eric Mitchell, Christopher D. Manning, Stefano Ermon, and Chelsea Finn. Direct preference optimization: Your language model is secretly a reward model. In *NeurIPS*, 2023.
- [22] John Schulman, Filip Wolski, Prafulla Dhariwal, Alec Radford, and Oleg Klimov. Proximal policy optimization algorithms. *CoRR*, abs/1707.06347, 2017.
- [23] Krista Opsahl-Ong, Michael J. Ryan, Josh Purtell, David Broman, Christopher Potts, Matei Zaharia, and Omar Khattab. Optimizing instructions and demonstrations for multi-stage language model programs. In *EMNLP*. Association for Computational Linguistics, 2024.
- [24] Petro Liashchynskyi and Pavlo Liashchynskyi. Grid search, random search, genetic algorithm: A big comparison for NAS. *CoRR*, abs/1912.06059, 2019.
- [25] Qingyan Guo, Rui Wang, Junliang Guo, Bei Li, Kaitao Song, Xu Tan, Guoqing Liu, Jiang Bian, and Yujiu Yang. Connecting large language models with evolutionary algorithms yields powerful prompt optimizers, 2024. URL <https://arxiv.org/abs/2309.08532>.
- [26] Noah Shinn, Federico Cassano, Ashwin Gopinath, Karthik Narasimhan, and Shunyu Yao. Reflexion: language agents with verbal reinforcement learning. In *NeurIPS*, 2023.
- [27] Yang Yu, Qiyue Yin, Junge Zhang, Pei Xu, and Kaiqi Huang. ADMN: agent-driven modular network for dynamic parameter sharing in cooperative multi-agent reinforcement learning. In *Proceedings of the Thirty-Third International Joint Conference on Artificial Intelligence, IJCAI 2024, Jeju, South Korea, August 3-9, 2024*. ijcai.org, 2024.
- [28] Xunjian Yin, Xinyi Wang, Liangming Pan, Xiaojun Wan, and William Yang Wang. Gödel agent: A self-referential agent framework for recursive self-improvement, 2025. URL <https://arxiv.org/abs/2410.04444>.
- [29] Changyu Chen, Zichen Liu, Chao Du, Tianyu Pang, Qian Liu, Arunesh Sinha, Pradeep Varakantham, and Min Lin. Bootstrapping language models with dpo implicit rewards. In *International Conference on Learning Representations (ICLR)*, 2025.
- [30] Shunyu Yao, Jeffrey Zhao, Dian Yu, Nan Du, Izhak Shafran, Karthik R. Narasimhan, and Yuan Cao. React: Synergizing reasoning and acting in language models. In *ICLR*, 2023.
- [31] Jiayi Zhang, Jinyu Xiang, Zhaoyang Yu, Fengwei Teng, Xionghui Chen, Jiaqi Chen, Mingchen Zhuge, Xin Cheng, Sirui Hong, Jinlin Wang, Bingnan Zheng, Bang Liu, Yuyu Luo, and Chenglin Wu. Aflow: Automating agentic workflow generation, 2025. URL <https://arxiv.org/abs/2410.10762>.
- [32] Wanxia Zhao, Mert Yuksekogun, Shirley Wu, and James Zou. Sirius: Self-improving multi-agent systems via bootstrapped reasoning, 2025.
- [33] Kunyang Lin, Yufeng Wang, Peihao Chen, Runhao Zeng, Siyuan Zhou, Minghui Tan, and Chuang Gan. Dcir: Dynamic consistency intrinsic reward for multi-agent reinforcement learning, 2023. URL <https://arxiv.org/abs/2312.05783>.

- [34] Yiqun Chen, Lingyong Yan, Weiwei Sun, Xinyu Ma, Yi Zhang, Shuaiqiang Wang, Dawei Yin, Yiming Yang, and Jiaxin Mao. Improving retrieval-augmented generation through multi-agent reinforcement learning. *CoRR*, 2025.
- [35] Jiaao Chen, Aston Zhang, Xingjian Shi, Mu Li, Alex Smola, and Diyi Yang. Parameter-efficient fine-tuning design spaces, 2023. URL <https://arxiv.org/abs/2301.01821>.
- [36] Zhaozhi Wang, Kefan Su, Jian Zhang, Huizhu Jia, Qixiang Ye, Xiaodong Xie, and Zongqing Lu. Multi-agent automated machine learning. In *IEEE/CVF Conference on Computer Vision and Pattern Recognition, CVPR 2023, Vancouver, BC, Canada, June 17-24, 2023*. IEEE, 2023.
- [37] Stefan Falkner, Aaron Klein, and Frank Hutter. BOHB: Robust and efficient hyperparameter optimization at scale. In Jennifer Dy and Andreas Krause, editors, *Proceedings of the 35th International Conference on Machine Learning*, volume 80 of *Proceedings of Machine Learning Research*, pages 1437–1446. PMLR, 10–15 Jul 2018. URL <https://proceedings.mlr.press/v80/falkner18a.html>.
- [38] Hieu Pham, Melody Guan, Barret Zoph, Quoc Le, and Jeff Dean. Efficient neural architecture search via parameters sharing. In Jennifer Dy and Andreas Krause, editors, *Proceedings of the 35th International Conference on Machine Learning*, volume 80 of *Proceedings of Machine Learning Research*, pages 4095–4104. PMLR, 10–15 Jul 2018.
- [39] Hanxiao Liu, Karen Simonyan, and Yiming Yang. Darts: Differentiable architecture search, 2019. URL <https://arxiv.org/abs/1806.09055>.
- [40] Hunter Lightman, Vineet Kosaraju, Yuri Burda, Harrison Edwards, Bowen Baker, Teddy Lee, Jan Leike, John Schulman, Ilya Sutskever, and Karl Cobbe. Let’s verify step by step. In *ICLR*, 2024.
- [41] Jonathan Uesato, Nate Kushman, Ramana Kumar, H. Francis Song, Noah Y. Siegel, Lisa Wang, Antonia Creswell, Geoffrey Irving, and Irina Higgins. Solving math word problems with process- and outcome-based feedback. *CoRR*, abs/2211.14275, 2022.
- [42] Shuaijie She, Junxiao Liu, Yifeng Liu, Jiajun Chen, Xin Huang, and Shujian Huang. R-prm: Reasoning-driven process reward modeling, 2025. URL <https://arxiv.org/abs/2503.21295>.
- [43] Teng Wang, Zhangyi Jiang, Zhenqi He, Wenhan Yang, Yanan Zheng, Zeyu Li, Zifan He, Shenyang Tong, and Hailei Gong. Towards hierarchical multi-step reward models for enhanced reasoning in large language models, 2025. URL <https://arxiv.org/abs/2503.13551>.
- [44] Peiyi Wang, Lei Li, Zhihong Shao, Runxin Xu, Damai Dai, Yifei Li, Deli Chen, Yu Wu, and Zhifang Sui. Math-shepherd: Verify and reinforce llms step-by-step without human annotations. In *ACL*, pages 9426–9439. Association for Computational Linguistics, 2024.
- [45] Yiran Ma, Zui Chen, Tianqiao Liu, Mi Tian, Zhuo Liu, Zitao Liu, and Weiqi Luo. What are step-level reward models rewarding? counterintuitive findings from mcts-boosted mathematical reasoning, 2025. URL <https://arxiv.org/abs/2412.15904>.
- [46] Fangkai Jiao, Chengwei Qin, Zhengyuan Liu, Nancy F. Chen, and Shafiq Joty. Learning planning-based reasoning with trajectory collection and process rewards synthesizing. In *EMNLP*. Association for Computational Linguistics, 2024.
- [47] Guoxin Chen, Minpeng Liao, Chengxi Li, and Kai Fan. Step-level value preference optimization for mathematical reasoning. In *Findings of the Association for Computational Linguistics: EMNLP 2024*, 2024.
- [48] Amrith Setlur, Chirag Nagpal, Adam Fisch, Xinyang Geng, Jacob Eisenstein, Rishabh Agarwal, Alekh Agarwal, Jonathan Berant, and Aviral Kumar. Rewarding progress: Scaling automated process verifiers for LLM reasoning. *ICLR*, 2025.
- [49] Zhenfang Chen, Delin Chen, Rui Sun, Wenjun Liu, and Chuang Gan. Scaling autonomous agents via automatic reward modeling and planning, 2025. URL <https://arxiv.org/abs/2502.12130>.

- [50] Sanjiban Choudhury. Process reward models for llm agents: Practical framework and directions, 2025. URL <https://arxiv.org/abs/2502.10325>.
- [51] Yilun Jin, Zheng Li, Chenwei Zhang, Tianyu Cao, Yifan Gao, Pratik Jayarao, Mao Li, Xin Liu, Ritesh Sarkhel, Xianfeng Tang, et al. Shopping mmlu: A massive multi-task online shopping benchmark for large language models. *arXiv preprint arXiv:2410.20745*, 2024.
- [52] Qiao Jin, Bhuwan Dhingra, Zhengping Liu, William Cohen, and Xinghua Lu. Pubmedqa: A dataset for biomedical research question answering. In *EMNLP-IJCNLP*, 2019.
- [53] National Center for Biotechnology Information (NCBI). PubMed. <https://pubmed.ncbi.nlm.nih.gov/>, 2024. Accessed: 2025-05-07.
- [54] Shirley Wu, Shiyu Zhao, Michihiro Yasunaga, Kexin Huang, Kaidi Cao, Qian Huang, Vassilis N. Ioannidis, Karthik Subbian, James Zou, and Jure Leskovec. Stark: Benchmarking llm retrieval on textual and relational knowledge bases. In *NeurIPS Datasets and Benchmarks Track*, 2024.
- [55] Zhilin Yang, Peng Qi, Saizheng Zhang, Yoshua Bengio, William W Cohen, Ruslan Salakhutdinov, and Christopher D Manning. Hotpotqa: A dataset for diverse, explainable multi-hop question answering. *EMNLP*, 2018.
- [56] Terry Yue Zhuo, Minh Chien Vu, Jenny Chim, Han Hu, Wenhao Yu, Ratnadira Widyasari, Imam Nur Bani Yusuf, Haolan Zhan, Junda He, Indraneil Paul, et al. Bigcodebench: Benchmarking code generation with diverse function calls and complex instructions. *arXiv preprint arXiv:2406.15877*, 2024.
- [57] Hoang Minh Le, Nan Jiang, Alekh Agarwal, Miroslav Dudík, Yisong Yue, and Hal Daumé III. Hierarchical imitation and reinforcement learning. In *ICML*, 2018.
- [58] Paul Tseng. Convergence of a block coordinate descent method for nondifferentiable minimization. *Journal of optimization theory and applications*, 109:475–494, 2001.

A Theoretical Analysis

Formal statement of and proof of Theorem 4.1 According to the procedure described in Section 4, the positive and negative pairs are determined by comparing the expected task metrics. We assume the estimated metrics at y_k^+ and y_k^- are chosen following $\mathbb{P}(y_k^+ \text{ is labeled as positive}) = \sigma_\alpha(\mathbb{E}_{\text{downstream}}[R(x, f(x; \mathbf{v}_{-k}(x))) \mid y_k^+] - \mathbb{E}_{\text{downstream}}[R(x, f(x; \mathbf{v}_{-k}(x))) \mid y_k^-])$, where $\sigma_\alpha(u) = \frac{1}{1 + \exp(-\alpha u)}$ is the sigmoid function with parameter $\alpha > 0$. $\alpha = +\infty$ corresponds to the case where the pairs are chosen deterministically.

Theorem A.1. *Under the conditions specified above, the maximizer of (5) satisfies the local-global alignment property (4). In addition, maximizing $r_k(x, C_k(x_k; \mathbf{v}_k))$ over v_k and maximizing $R(x, f(x; \mathbf{v}_{-k}) \mid C_k(x_k; \mathbf{v}_k))$ over v_k will yield the same solution.*

Proof. We first present a lemma.

Lemma A.1. *Suppose $(\mathbf{x}, y) \in \mathbb{R}^p \times \{-1, 1\}$ follows the distribution $\mathbb{P}(y = 1 \mid \mathbf{x}) = \sigma_1(p^*(x))$ for some function $p : \mathbb{R}^p \rightarrow (0, 1)$. Then*

$$\arg \min_p \mathbb{E}[\log(\sigma_1(y \cdot p(x)))] = p^*.$$

Proof. We take the derivative of the left-hand side with respect to p and set it to 0:

$$\mathbb{E}\left[\frac{\sigma_1(y \cdot p(x)) \cdot \sigma_1(-y \cdot p(x))}{\sigma_1(y \cdot p(x))} \cdot y\right] = 0,$$

which is equivalent to

$$\mathbb{E}[\sigma_1(-y \cdot p(x)) \cdot y] = 0.$$

We then have

$$\sigma_1(-p(x))\sigma_1(p^*(x)) - \sigma_1(p(x))\sigma_1(-p^*(x)) = 0,$$

and therefore $p(x) = p^*(x)$. □

Applying this lemma, we can obtain the solution to (5) is $\alpha \cdot \mathbb{E}_{\text{downstream}}[R(x, f(x; \mathbf{v}_{-k}(x))) \mid y_k]$ for some positive α , and therefore it satisfies the local-global alignment property.(4)

In the following, we then prove that maximizing $r_k(x, \pi_k(x))$ over v_k and maximizing $R(x, f(x; \mathbf{v}_{-k}) \mid \pi_k(x))$ over v_k will yield the same solution.

Lemma A.2. *Assume the local-global alignment property (4) holds for component C_k . Let $\mathbf{v}(x)$ and $\tilde{\mathbf{v}}(x)$ be two configuration policies that differ only in the policy for component C_k ; denote the corresponding local outputs by y_k and \tilde{y}_k , respectively. If*

$$\mathbb{E}_x[r_k(x_k, \tilde{y}_k)] > \mathbb{E}_x[r_k(x_k, y_k)],$$

then

$$\mathbb{E}_x[R(x, f(x; \tilde{\mathbf{v}}(x)))] \geq \mathbb{E}_x[R(x, f(x; \mathbf{v}(x)))] .$$

Proof. Fix an arbitrary input instance x . Because the two policies differ only at C_k , all other component configurations remain the same, so we can write

$$f(x; \mathbf{v}_{-k}(x), y_k) \quad \text{and} \quad f(x; \mathbf{v}_{-k}(x), \tilde{y}_k),$$

where $\mathbf{v}_{-k}(x)$ denotes downstream configurations (independent of the choice at C_k). By assumption on the expected local reward, we have $r_k(x_k, \tilde{y}_k) \geq r_k(x_k, y_k)$ for almost every x . Applying the alignment property (4) pointwise yields

$$\mathbb{E}_{\text{downstream}}[R(x, f(x; \mathbf{v}_{-k}(x), \tilde{y}_k)) \mid x_k] \geq \mathbb{E}_{\text{downstream}}[R(x, f(x; \mathbf{v}_{-k}(x), y_k)) \mid x_k].$$

Taking the expectation over x (law of total expectation) gives

$$\mathbb{E}_x[R(x, f(x; \tilde{\mathbf{v}}(x)))] \geq \mathbb{E}_x[R(x, f(x; \mathbf{v}(x)))] .$$

Hence increasing the expected local reward for C_k cannot decrease—and may strictly increase—the expected global objective. □

□

Proof of Theorem 4.2 We first show that the algorithm is essentially performing coordinate maximization on $l(\mathbf{v})$. In fact, given a previous configuration \mathbf{v}^t , at time t , the updated configuration \mathbf{v}^{t+1} only changes the configuration of a single component, say, C_k . As the change is solved by maximizing $r_k(x, C_k(x_k; \mathbf{v}_k))$, by Theorem 4.1, this is equivalently maximizing $l(\mathbf{v}_k, \mathbf{v}_{-k})$ for the k -th coordinate.

To rule out cycling, we first prove that the discrete block $\mathbf{v}^{(2)}$ stabilizes. Consider the sequence $(\mathbf{v}^{1,(1)}, \mathbf{v}^{1,(2)}), (\mathbf{v}^{2,(1)}, \mathbf{v}^{2,(2)}), \dots, (\mathbf{v}^t, (1), \mathbf{v}^t, (2)), \dots$. We first show that there exists $T > 0$, such that for all $k > 0$, $\mathbf{v}^{T+k, (2)} = \mathbf{v}^{T, (2)}$.

As $\mathbf{v}^{(2)}$ are discrete, there are finitely many different configurations. In addition, according to the assumption that the coordinate-wise maximum is unique, each update will result in a strict decrease in the loss function. Therefore, after finite number of iterations, $\mathbf{v}^{(2)}$ will not change.

Now when we consider all the iterations that are later than the time T , $\mathbf{v}^{(2)}$ is fixed, and we only need to consider the update regarding $\mathbf{v}^{(1)}$. In this case, we apply Theorem 4.1 of [58] and complete the proof.

B Dataset Details

This appendix provides the essential statistics and source information for the five compound-system benchmarks used in our experiments (Figure 2). For each dataset we specify the train / validation / test split sizes, the task formulation as used in the compound pipeline, and the evaluation metric reported in the main paper

AMAZON (Behavior-Driven Next-Item Recommendation). The corpus is derived from Amazon product-interaction logs released by Jin et al. [51]. Each instance consists of a user’s historical behaviour sequence (views, clicks, purchases) and the target “next item” to be recommended. We split it into to 335 / 60 / 99 user sequences after filtering malformed entries. Accuracy - whether the predicted item number 1 matches the ground truth - is the evaluation metric.

PUBMEDQA (Medical Analysis based QA). PUBMEDQA [52] contains biomedical abstracts paired with yes/no/maybe answers to research questions. We keep the original “expert” split and discard ambiguous samples, resulting in 475 / 25 / 500 question–abstract pairs. Our compound system frames the task as three-way classification; exact-match accuracy is reported.

STARK-PRIME (Semi-Structured Knowledge Base Retrieval). STARK-PRIME -Prime originates from STARK benchmark introduced by Wu et al. [54]. It blends free-text passages with relational triples from biomedical knowledge graphs. Queries are natural-language questions; relevance labels are automatically propagated from the original STARK annotations. We uses the original dataset split: 495 / 51 / 96 queries. Performance is measured by Hit@1, which is the rate of ranking the ground truth items in the predicted ranking list.

HOTPOTQA (Retrieval-Augmented Multi-Hop QA). We adopt the HOTPOTQA [55] and keep the official train/dev/test splits: 1000, 250, and 100 questions respectively. Each example in the set contains a question and its (human-annotated) answer. We report answer-level F1 score.

BIGCODEBENCH (Self-Verified Code Generation). We use a subset of the *full-instruction* subset of BigCodeBench [56] due to efficiency issue. After proportionally drop the data, we obtain 500 / 25 / 70 coding tasks. Each sample includes a natural-language specification and reference unit tests. Our metric is *pass@1*: the proportion of generated programs that pass all tests in one try.

C Compound AI System Details

Table 5 summarizes each pipeline’s modules (columns: *System*, *Module*, *Model*, *Config*, and *Optimization*). In the table below, we clarify the various configuration spaces and optimization methods used across the five systems.

Table 5: Modules, models, and optimization methods. *Model Selection (LLMs)*¹ indicates a discrete choice of LLMs. *Aggregator*² is tuned over coefficients `relation_weight` and `text_weight`. *Retriever*³ has a hyperparameter `k`.

System	Module	Model	Config	Optimization
Amazon	Session Analyzer	Qwen 2.5 1B	Model Params	PPO (RL)
	Candidate Profiler	Qwen 2.5 1B	Model Params	PPO (RL)
	Next Item Decider	GPT-4o-mini	Prompt	Prompt Opt.
PubMed	Context Model Selector	–	Model Selection (LLMs) ¹	Hyperparam Search
	Context Analyst	One of {gpt-4o, ...} ¹	Prompt	Prompt Opt.
	Solver Model Selector	–	Model Selection (LLMs) ¹	Hyperparam Search
	Problem Solver	One of {gpt-4o, ...} ¹	Prompt	Prompt Opt.
STaRK	Text Scorer	Claude 3 Haiku	Prompt	Prompt Opt.
	Relation Scorer	Claude 3 Haiku	Prompt	Prompt Opt.
	Aggregator ²	–	Coefficients	Hyperparam Search
HotpotQA	Question Rewriter	GPT-4o-mini	Prompt	Prompt Opt.
	Info Extractor	GPT-4o-mini	Prompt	Prompt Opt.
	Retriever ³	–	#Retrieved passages	Hyperparam Search
	Hint Generator	GPT-4o-mini	Prompt	Prompt Opt.
	Answer Generator	GPT-4o-mini	Prompt	Prompt Opt.
BigCodeBench	Code Generator	Claude 3 Haiku	Prompt	Prompt Opt.
	Unit Test Generator	Claude 3 Haiku	Prompt	Prompt Opt.
	Final Code Generator	Claude 3 Haiku	Prompt	Prompt Opt.

AMAZON (Behavior-Driven Next-item Recommendation). *Session Analyzer* and *Candidate Profiler* both use the Qwen 2.5 1B model; we optimize their model parameters with PPO reinforcement learning [22]. This helps each module better encode task-specific knowledge, *i.e.*, user sessions and product candidates. The final *Next Item Decider* is a GPT-4o-mini module, whose *prompt* we optimize.

PUBMEDQA (Medical Analysis based QA). Two modules (*Context Model Selector* and *Solver Model Selector*) each do discrete model selection from a *list of possible LLMs*. At inference time, these selectors use a reward model to pick the best LLM for each input instance. The *Context Analyst* and *Problem Solver* modules then receive the chosen model and optimize *only the prompt* for improved medical QA performance.

STARK-PRIME (Semi-Structured KB Retrieval). We have two scoring modules (*Text Scorer*, *Relation Scorer*), both using Claude 3 Haiku with *prompt optimization*. The *Aggregator* merges these two scores; we tune two numeric weights, `relation_weight` and `text_weight`, each set in $\{0.1, 1.0\}$. We perform a global hyperparameter search across the entire training set for the *Aggregator* module, tuning `relation_weight` and `text_weight`. After identifying the best fixed combination, we use it in for inference.

HOTPOTQA (Retrieval-Augmented Multi-Hop QA). Four GPT-4o-mini modules (*Question Rewriter*, *Info Extractor*, *Hint Generator*, *Answer Generator*) each rely on *prompt optimization* to improve multi-hop reasoning. Meanwhile, the *Retriever* is retriever with a key hyperparameter `k`, the number of passages to pull. We search $k \in \{1, 5, 10, 25\}$ which we also tune via global hyperparameter search across training instances.

BIGCODEBENCH (Self-Verified Code Generation). All three modules (*Code Generator*, *Unit Test Generator*, *Final Code Generator*) are Claude 3 Haiku LLMs; each uses *prompt optimization* to iteratively refine code solutions based on test outcomes. The global objective is a higher pass rate on the final code.

¹**Model Selection (LLMs):** we search over {gpt-4o, gpt-4o-mini, gpt-3.5-turbo-0125, gpt-4-turbo, claude-3-5-haiku-20241022, claude-3-5-sonnet-20241022, claude-3-7-sonnet-20250219}.

²**Aggregator (STaRK):** we search `relation_weight, text_weight` $\in \{0.1, 1.0\}$.

³**Retriever (HotpotQA):** we search `k` $\in \{1, 5, 10, 25\}$.

Overall, the table illustrates how **different modules can require different types of optimization**—from prompt tuning (textual modifications) and model-parameter fine-tuning (PPO) to discrete model selection and hyperparameter search. By unifying these heterogeneous updates within our OPTIMAS framework, we effectively coordinate local improvements to achieve consistent global reward gains.

All experiments were run on a node with 8 NVIDIA A100 GPUs (80 GB memory each); depending on the complexity of the compound system and hyperparameters, training and optimization typically finished in 2–8 hours.

Table 6: Key hyperparameters for the local reward model training.

Parameter	Value
Base model	Llama 3 8B Instruct
LoRA rank	32
LoRA alpha	16
Maximum sequence length	2048 tokens
Learning rate	2e-6
Number of epochs	25
batch size	32

Before on-policy optimization, we train a reward model on preference pairs (“chosen” vs. “rejected” system outputs) so it can assign higher scores to better outputs. Table 6 highlights the main hyperparameters for this stage. We adopt LoRA for memory efficiency, and use an early-stopping mechanism based on the evaluation loss (patience=512 steps) to reduce overfitting.

After training the reward model, we run iterative on-policy optimization for each module in the compound AI system. Table 7 lists the key hyperparameters. For example, the *train size* (50) limits how many examples are used to train each module’s local configuration, while the *search size* (50) sets how many samples we use when searching for the best local update. When a module is selected, we collect a small preference data, retrain (or adapt) the reward model as needed, then locally optimize that module’s parameters or prompts to maximize its local reward.

Table 7: Key hyperparameters for on-policy optimization.

Parameter	Value / Description
Train size	50
Search size	50
Prompt candidates	3
Local optimization steps	3
Fresh input size	20
Validation size	20

D Baseline Details

We provide the details to reproduce the reported baseline results and the results of OPTIMAS.

- **LLMSelector:** We run LLMSelector [8] with the LLMDIAGNOSER to estimate per-module performance, following their procedure. We perform two rounds of allocation updates with 100 training examples each round.
- **Hierarchical Behavior Cloning (HBC):** We run HBC using the collected preference dataset by replacing the original reward model with the embedding similarity score. With the same input in the preference dataset, we use `text-embedding-3-small` to embed the module output and the preferred output in the preference dataset and calculate the embedding similarity score. We further weight the similarity score using the gap of the preferred output score and the rejected output score to get the reward for HBC.
- **TextGrad:** We run TextGrad using GPT-4o mini to optimize each component’s prompt independently in separate epochs. Validation is performed every two optimization steps using 20 held-out validation instances. A batch size of 4 is used across all components and datasets. The

best-performing prompt, as determined by validation frequency of LLM-generated textual feedback, is selected as the final configuration.

- **DSPy:** We conduct optimization on DSPy’s MIPRO [23] prompt optimization approach. For fair comparison, we disable the few-shot example and system prompt optimization and only conducts optimization on the user instructions. We dynamically set the number of iterations for the MIPRO optimizer to match the budget of system runs in Table 3.

For TextGrad, DSPy, and OPTIMAS, we consistently using the same 20 held-out validation instances on each dataset to select the best configurations.

E OPTIMAS Details

We provide open access to our implementation code, including the Optimas framework and the compound system implementations for all five benchmarks at <https://anonymous.4open.science/r/optimas-1308/>.

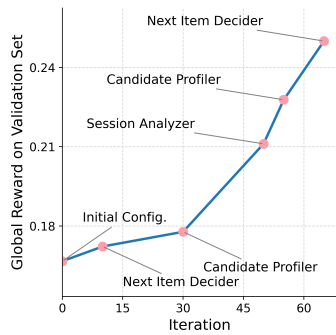
Component selection. At each iteration t , we select a component to optimize. The selection can be made uniformly at random, or guided by a heuristic that prioritizes components likely to be performance bottlenecks. Specifically, for each component, we compute the average difference in expected global rewards between preferred and non-preferred outputs in its previous preference data. This value reflects the potential impact of improving the component, and we sample one for optimization with probability proportional to its average metric gap.

Local Optimization Steps for Different Configurations. Since each component controls only one configuration type, we can tailor the optimization approach as follows:

- **Prompt tuning.** For textual prompts, we apply prompt optimization algorithms [17, 19], using r_k as the evaluation metric. We sample multiple prompts limited by a max number of prompt candidates. The prompts are ranked by average reward over validation instances, and the best-performing prompt is selected.
- **Model fine-tuning.** When C_k is an LLM or neural model with trainable parameters, we can apply reinforcement learning algorithms, such as Proximal Policy Optimization (PPO) [22], using r_k as the critic. The model parameters are updated for a small and fixed number of steps.
- **Model selection and hyperparameter tuning.** For discrete or low-dimensional continuous configurations, such as model selection, tool routing, or scalar hyperparameters, we formulate the optimization as a sampling problem parameterized by a probabilistic distribution. Since these configurations are instance-specific, the expectation in Eq. (7) reduces to a single input. For each input x , we evaluate a set of candidate configurations using the LRF r_k , and compute a probability distribution over candidates proportional to $\exp\{r_k(x_k, C_k(x_k; \mathbf{v}_k))\}$. This distribution is then used to sample the configuration update for the current iteration.

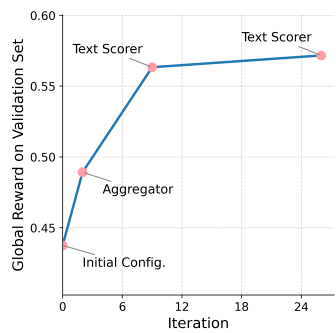
Under a conservative update to the configuration of a component C_k , the expected global reward is guaranteed to maintain or improve, if the local–global alignment property in Eq. (4) holds.

F More Experiment Results



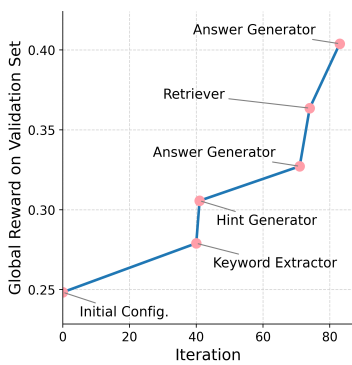
Optimized Component	Config. type	Configuration Before	Configuration After
Next Item Decider	Prompt	Pick the next item based on summary + feedback.	Based on the provided summary and feedback, select the next item that best aligns with the user's preferences and recommendations. Ensure that your choice reflects the desired characteristics outlined in the summary, while incorporating any constructive feedback received.
	Model Parameters	< Model parameter change >	
	Model Parameters		
Next Item Decider	Prompt	Based on the provided summary and feedback, select the next item that best aligns with the user's preferences and recommendations. Ensure that your choice reflects the desired characteristics outlined in the summary, while incorporating any constructive feedback received.	Analyze the provided context (summary of user browsing behavior) and feedback (item-by-item assessments) to determine which candidate item the user is most likely to engage with next in their e-commerce session. Return only the index number of the chosen item. Consider how well each item aligns with the detected user intent from the context and the specific strengths/weaknesses noted in the feedback. Prioritize items that complement rather than duplicate what the user has already viewed.

(a) AMAZON system



Optimized Component	Config. type	Configuration Before	Configuration After
Aggregator	Hyperparameter	{'relation_weight': 0.1, 'text_weight': 0.1}	{'relation_weight': 1.0, 'text_weight': 0.1}
Text Scorer	Prompt	Given a question and a list of 5 entities with their property information, assign each entity a relevance score between 0 and 1 based on how well its properties match the requirements described in the question.	You are tasked with assessing the relevance of five entities based on a specific question. For each entity, carefully analyze its properties in relation to the question's requirements. Assign a relevance score from 0 to 1, where 0 means no relevance and 1 means complete relevance. Please provide a brief justification for each score, highlighting both direct matches and any relevant implicit connections. Strive for clarity and precision to ensure that the scores accurately reflect the entities' relevance to the question.
Text Scorer	Prompt	~(Same as "Configuration After" in the last row)	Given a question and a list of 5 entities, each with detailed property information, assign a relevance score between 0 and 1 to each entity based on the following criteria:

(b) STARK-PRIME system



Optimized Component	Config. type	Configuration Before	Configuration After
Keyword Extractor	Prompt	Extract keywords from the query to retrieve relevant content.	Extract the essential keywords and phrases from the following query to enhance content retrieval. Focus on the most impactful terms that represent the main idea.
Hint Generator	Prompt	Generate useful hints to answer the query.	Generate relevant and actionable hints to effectively address the given query, ensuring clarity and conciseness in your responses.
Answer Generator	Prompt	Given some hints, directly answer the query with a short answer for the query.	Given 3 to 5 clear and relevant hints, provide a direct and concise answer to the query in no more than 10 words. Your response should strictly focus on the question without any additional context or elaboration. If the hints are ambiguous, unclear, or insufficient to formulate an answer, clearly indicate that more information is needed for a proper response.
Retriever	Hyperparameter	(number of retrieved passages) k=1	k=5
Answer Generator	Prompt	Given 3 to 5 clear and relevant hints, provide a direct and concise answer to the query in no more than 10 words. Your response should strictly focus on the question without any additional context or elaboration. If the hints are ambiguous, unclear, or insufficient to formulate an answer, clearly indicate that more information is needed for a proper response.	Please provide a clear and direct answer to the following query, using the hints. Limit your response to 5 words or less, and include any relevant numerical data. Avoid any additional explanations or context.

(c) HOTPOTQA system

Figure 7: Configuration updates during OPTIMAS optimization on three compound AI systems: AMAZON, HOTPOTQA, and STARK-PRIME .